Title

Customizing the surface charge and performance of thin-film composite membranes by plasma polymerization

Authors

Rackel Reis[1,2], Mikel Duke[1], Andrea Merenda[2], Bjorn Winther-Jensen[3], Ljiljana Puskar[4], Mark J. Tobin[5], John D. Orbell[1] and Ludovic F. Dumée[2#]

Affiliations

[1] Victoria University, Institute for Sustainability and Innovation, Hoppers Lane, Werribee 3030, Victoria, Australia

[2] Deakin University, Geelong, Pigdons Road Institute for Frontier Materials, Waurn Ponds 3216, Victoria, Australia

[3] Waseda University, Department of Advanced Science and Engineering, Tokyo, Japan

[4] Helmholtz-Zentrum Berlin für Materialien und Energie GmbH Methoden der Materialentwicklung, D-12489 Berlin, Germany

[5]Australian Synchrotron, 800 Blackburn Road, Clayton 3168, Victoria, Australia

#Corresponding author: Ludovic.dumee@deakin.edu.au; +61 4 1013 1312

Abstract

Solute-surface interactions are critical in membrane science and dominate a number of diffusion and selectivity parameters. In water treatment particularly, the charge on the membrane has been shown to affect ion transport selectivity as well as fouling mechanisms. The development of advanced surface technologies that allow for potential customization of the surface charge for specific applications, without compromising the essential performance of the membrane, is therefore desirable. In this paper, a novel plasma polymerization strategy was applied to commercial reverse osmosis membrane in order to tune the surface charge. Two monomers, maleic anhydride and vinylimidazole, were plasma polymerized onto the membrane resulting in a modification of the surface energy with resultant iso-electric points of approx. pH 3 and pH 7 respectively. This required only a short 5 min plasma polymerization treatment in each case. Thus, in addition to enhancing the water permeation by up to 10 %, in comparison to the reference membranes, the overall charge of the membranes was shifted from highly negatively charged upon maleic anhydride polymerization to highly positively charged upon vinylimidazole polymerization. A comprehensive morphological and chemical analysis was performed to correlate the changes to the presence of functional groups and the alteration of the surface texture. Short treatments were found to smooth the surface whilst enriching the surface with either carboxylic or amine/amide groups. This work opens new avenues to engineer advanced membranes with improved performance and selectivity.

Keywords

Charge control; thin film composite membranes; plasma polymerization; surface deposition

1. Introduction

The surface properties of reverse osmosis (RO) thin-film composite (TFC) membranes are of fundamental importance in order to produce high water quality and to control both surface interactions and deposition mechanisms [1]. The ability of the membrane to reject dissolved salts is dependent on the charge of the surface and, therefore, on the polarizability of the functional groups present at the liquid/solid interface [2, 3]. The pH of the solution in contact with the membrane will dictate the hydronium and hydroxyl ion concentrations and the charge environment within the Stern layer, thus affecting which ions are repelled or attracted by electrostatic forces [4, 5]. The charge density, polarity and isoelectric points (IEP), as well as the roughness and exposed surface area of the membrane, therefore play a significant role in species rejection [6, 7]. Control of the surface charge and polarizability parameters is regularly highlighted as critical for suitable wastewater treatment or management in order to maintain membrane performance during operation [8]. In addition to the native poly(amide)(PA) material, commercial reverse osmosis (RO) membranes also often incorporate a protective proprietary hydrophilic coating, to limit the adverse effect of fouling on the long term operation of these materials [9].

Plasma polymerization technologies offer advanced platforms for a rapid surface functionalization, allowing for the simultaneous tuning of surface energy and morphology [10, 11]. The morphology of TFC membranes makes them, however, vulnerable to surface reactions and degradation. New routes to engineer customized surfaces properties of TFC membrane materials for specific applications and effluents, without compromising the integrity of the selective layer, are required. To date, most of the plasma surface modifications of membrane materials have involved the use of radio frequency (RF), low pressure, plasma generation to induce chemical polymerization and deposition [12, 13]. However RF plasma generators are highly energetic and yield large densities of activated radical species, thus generating harsh conditions

that can result in degradation of both substrate and monomer molecules [14, 15]. The drying process induced at low pressure may cause capillary stresses and collapse across the pores of the PA or underlining layers within the membrane material and ultimately compromise liquid permeability [16-18]. The ultra-thin PA layer across the TFC membranes was previously shown to be compromised by surface etching mechanisms even at low working powers and plasma glow intensities [10] and, in such conditions, the water flux was previously shown to be severely reduced by up to 70% [19]. Besides, polymerization - deposition mechanisms typically lead to a high degree of branching and crosslinking of the monomer molecules and, therefore, to low control of the free volume density and overall microstructure of the material [20]. Low frequency alternating current (AC) systems on the other hand offer higher control in terms of both deposition kinetics and chemical activation since they are typically operated with much lower carrier gas pressures [20]. Monomer molecules may therefore be primed and activated by the AC plasma during the polymerization process leading to better defined macromolecular structures and degrees of cross-linking[21]. The control and investigation of polymerized layers across the membrane surfaces may, however, be controlled down to the nanoscale and shows promise for the customization of the charge density and polarizability of TFC membranes [22].

In this work, a novel strategy was investigated for the surface modification of commercial RO membranes, which led to (i) enhanced performance in terms of permeability/selectivity and (ii) unprecedented control over the surface charge of the material. The application of an AC low pressure plasma generator was explored to control the deposition of functional moieties across the commercial TFC membrane surface without washing off the nascent coating preservative layer prior to plasma treatment. The monomers, maleic anhydride (MA) and vinylimidazole (VIM), were employed to generate negative or positive charged ultra-thin coatings, respectively.

2. Experimental details

2.1 Materials and reagents

BW30 TFC membrane elements were purchased from Dow Filmtec Corp. (IMCD Australia Limited). The flat sheet membranes used in this work were collected from the same internal area of the element and stored in a dry environment at 4ºC. Analytical grade sodium chloride (NaCl) was purchased from Sigma Aldrich (Sydney, NSW, Australia) and used for the preparation of saline feed solution to give a concentration of 2,000 ppm. Milli-Q water was used for the preparation of all aqueous solutions. The monomers used for plasma polymerization, maleic anhydride (MA) and vinylimidazole (VIM), were purchased from Sigma Aldrich, 99% purity.

2.2 Plasma polymerization procedure

Plasma polymerization of the VIM and MA experiments were carried out separately following the same procedure as previously described elsewhere [19]. Membranes were placed separately into the low pressure AC vacuum chamber (reactor) (2 L) and firmly attached using a Scotch Magic® tape manufactured by 3M onto a plastic support - exposing the membrane active side only. A set of increasing plasma polymerization duration range was studied from 5, 9 and 15 min in both experiments with VIM and MA at fixed pressure of 7 Pa.

2.3 Characterization techniques

The morphology of the modified surfaces was evaluated by scanning electron microscopy. The scanning electron micrographs (SEM) were acquired on a FEI Quanta dual beam Gallium (Ga) Focused Ion Beam (FIB) microscope. The samples were coated with a 1-2 nm thick carbon layer prior to imaging. SEM were collected under 5 kV of accelerating voltage

and for a working distance of 10 mm. FIB cross sections were cut in 3 steps following a procedure previously described [23]. First an initial 1 nA current was used to mill a rough section and second the section was cleaned in two consecutive steps at 0.3 and 0.1 nA. The voltage of the Ga beam was constant at 30 kV and the working distance to match the eucentric height was 10 mm.

The surface charge of the modified membranes was evaluated in terms of the streaming potential with a Surpass Anton Paar, electro kinetic analyzer (EKA) with Visiolab software (version 2.2). The membranes were placed into a 20 mm × 10 mm adjustable gap cell. The streaming channel gap was set at approximately 0.10 +/- 0.01 mm. The maximum pressure used during the streaming potential evaluation was set at 500 mbar. Both conductivity and pH were systematically recorded to calculate the specific salts adsorption across the materials surfaces as a function of pH. A 1.10^{-2} M NaCl solution was used as streaming medium and either 0.1 M HCl or 0.1 M NaOH solutions were used for pH adjustment. An average value of the zeta potential was calculated based on four repeated measurements obtained by inverting the flow direction of the solution across the cell.

Attenuated total reflection - Fourier transform infrared spectroscopy (ATR-FTIR) tests were performed to investigate the chemical surface groups of the membranes and to analyze the potential surface reactions induced by the plasma polymerization. Single point ATR analysis of membrane samples was performed using a Perkin Elmer Frontier FTIR spectrophotometer with a KBr beam splitter and diamond crystal ATR accessory. All spectra were collected across a wavenumber range of 4000-600 cm^{-1} with a resolution of 4 cm^{-1}. 16 scans were performed per sample and analyzed by means of OPUS 7.2 software (Bruker). As plasma polymerization technique is well known for producing homogeneous and thin films coatings, the homogeneity of the polymerized functional groups on surface and film thickness after plasma polymerization was investigated using two dimensional FTIR maps were obtained

using the ATR-FTIR microscope accessory at the Australian Synchrotron IRM beamline. When The analysis was performed using a Bruker Hyperion 2000 microscope coupled to a V80v FTIR spectrometer, equipped with a narrow band 50 µm MCT detector and a Micro-ATR accessory (45º single reflection germanium ATR element) with a clean BaF_2 window used for collecting reference spectra. Total of 25 points were measured in each map using an aperture of 20 x 20 µm with spot size of 5 µm and distance between points of 2.5 µm. The FTIR map analyses investigated the distribution of crosslinking functional groups across the surface and estimated the amine and carboxylate rich coating thicknesses. The thickness was evaluated using the equation as described elsewhere [19], where absorbance intensity from new functionalities observed after plasma treatment was correlated according to the IR depth from the given frequency.

X-ray photoelectron spectroscopy (XPS) was utilized for elemental surface characterization. Measurements were performed using an XPS Spectrometer Kratos AXIS Nova (Kratos Analytical Ltd, Manchester, UK). A quantitative elemental composition of the modified PA was reaching down to a surface depth of 1–5 nm. The technique was able to detect elements with a detection limit of 0.1% of the bulk material. An Al Kα (1486.6 eV) X-ray source was used as the excitation source, where the anode was operated at 250 W, 10 kV, and 27 mA at a chamber pressure of 2.67×10^{-8} Pa and the emission focused to a beam spot size of 400 µm × 400 µm. The peak position was calibrated using the C1s peak at 284.5 eV.

2.4 Membrane desalination performance tests

Water permeation measurements in model saline water (NaCl 2,000 ppm at 25°C) were performed. The concentrated feed stream containing a saline solution was pumped to the system with an effective membrane area of 42 cm^2 and flowing tangentially across the

membrane surface under 15 bar, and trans-membrane pressures were monitored and maintained at the target working pressure within a +/- 2% accuracy. The outlet permeate flow was collected after 120 min and salt rejection conductivity measured immediately after the test. Salt concentration was determined using an electrical conductivity meter (Hach HQ40d) and mass of permeate was measured with a Metler MS40025/01 balance (+/- 0.001 mg). Salt rejection and water permeation performance were calculated as reported elsewhere [19]. The error bars for both flux and salt rejection for both control and plasma modified membranes corresponded to the standard estimated error of the mean.

3. Results and discussion

3.1 Surface morphology and chemical analysis

The degree of polymerization was initially assessed by SEM surface analysis. As shown in Figure 1, increased plasma polymerization process duration for both monomers led to a gradual smoothing of the surface and of the protrusions, visible on the pristine membranes (Figure S1). The coatings across the membrane materials appeared highly homogeneous and continuous. As previously shown for a similar system, the average surface roughness after plasma polymerization was found to reduce by 30% from 24 ± 0.2 nm (control) to 17 ± 0.4 nm after 15 min of plasma treatment, highlighting the impact of the plasma duration on the smoothing of the materials, as visible from the SEMs in Figure 1 [19].

The impact of duration on the plasma polymerization process was also investigated in terms of the resultant chemistry. Figure 2 presents FTIR spectra from the plasma polymerized membranes. In Figure 2A, the area of the band at 1666 cm^{-1} was chosen as a reference band corresponding to the C-N stretching vibration to assess amine enrichment by the VIM monomer after plasma polymerization, as also previously seen elsewhere [19]. The reference band was shown to increase with increasing duration of the polymerization process. Simultaneously, the intensity of the band at 1609 cm^{-1} corresponding to (N-H) deformation was found to be slightly enhanced after plasma polymerization [24, 25]. This may be correlated to pendant groups present across the polymerized VIM. Furthermore, a broad band at ~1720 cm^{-1} corresponding to a carbonyl (C=O) stretching vibration increased in intensity as a function of the plasma duration. The carbonyl band formed after plasma polymerization relates to the reaction of free radicals via atmospheric O_2, a common reaction found in polymers after plasma treatment [26]. Plasma polymerization of MA on the other hand, showed the formation of a broad band around 1722 cm^{-1} corresponding to C=O stretching vibration of carboxylate groups, the intensity of which was also enhanced increasing polymerization duration (Figure 2B). The contour colour FTIR

maps in Figure 2C, generated using integrated peaks at 1666 cm^{-1} (VIM) and 1722 cm^{-1} (MA) also confirmed the intensity increase of the functional groups as a function of the plasma duration. The thickness of these films was estimated based on evaluation of the penetration depth of the infra-red beam corresponding to the integrated wavelength area [19]. The absorbance of each integrated area from each spectra was averaged and used to estimate the thickness against the control sample. The estimated thickness of the amine film coverage after plasma polymerization of VIM was calculated at 31, 29 and 62 nm added to the surface, associated with increasing process durations of 5, 9 and 15 min, respectively. Similarly, for the MA polymerized samples, the estimated film thickness was found to be progressively increasing with respect to plasma duration. After 5 min of process duration the film thickness was estimated at 37 nm added to the surface, 20% above 5 min of duration obtained with amine enrichment with VIM. Furthermore, with 9 min of process duration film thickness was estimated at 102 nm, which are about 3 times higher than obtained with 9 min of the amine enrichment polymerization process. However, the estimated film thickness for polymerized membrane at 15 min of process duration was estimated at 83 nm which is 19% lower than of the 9 min polymerized membrane.

After 5 min of process duration the film polymerized thickness was estimated at 37 nm +/-2 nm prior to plateauing, within error of the calculation, upon reaching 9 min of process duration with the film thickness estimated to be 102 nm. On the FIB cross sections displayed in Figure 3, the homogeneous nature of the interface, as well as the continuity of the coatings can be clearly seen. The cross sections also reveal that the underlying poly(sulfone) materials were not apparently affected by the plasma treatment as expected from the mounting position of the membranes, facing the electrode, during operation. The larger thicknesses obtained for the MA polymerized samples suggest a faster polymerization kinetics which is consistent with a lower activation energy of the MA molecules compared to the VIM monomers to yield

polymerization. As the plasma conditions for both polymerization processes were the same, it may be assumed that the structural and electronic characteristics of the individual monomer molecules, such as their relative C-H homolytic bond dissociation energies, may influence their relative deposition rates onto the PA layer. Indeed, plasma polymerization hydrogen atom detachment within the monomer is reputed to play an important role in plasma polymerization yield [27, 28] The FTIR maps therefore demonstrate the continuous distribution of the polymerized moieties across the surface of the materials for both monomers and therefore the ability of the plasma polymerization process to homogeneously generate dense ultra-thin films.

The chemistry of the membranes was assessed by XPS analysis (Figure 4 and S2). The elemental XPS survey analysis of the VIM polymerized samples confirmed significant increase of N at%, upon polymerization (Table S1). The N/C ratio for the VIM polymerized samples was found to be constant across the series, supporting the fact that the extra polymerized layer, added over time, is intrinsically identical to the ones on which it is deposited (Figure 4A). The exact nature of the functional groups introduced by the radical polymerization was evaluated by fitting the C and N peaks (Figure 4B). The peak assignment was carried out considering previous work on imidazole polymerization and deposition or C-N bond formation in polymers[29]. The C 1s spectra was deconvoluted by taking into account the simultaneous presence of C-H, C-N, N-C=N and C=O bonds as can be inferred from the polymerization mechanism and the precursors involved. The functional groups were attributed to deconvoluted peaks appearing at 284.7, 285.6, 286.3 and 287.7 eV respectively [29, 30]. As for the N 1s high resolution spectra, the analysis focused on the deconvolution into two main curves corresponding to amine and imine functionalities, at 398.3 and 399.8 eV respectively [31]. In addition, the decrease of the hydroxyl density initially, may be therefore directly attributed to the physical etching by the plasma of that very thin preservative layer [32]. It is possible that the

presence of the preservative materials [33], which was not washed away in these tests, may have been reacted within the first few minutes of the plasma treatment.

The XPS analysis of the MA polymerized samples was also performed and is displayed in both Figure 4C and S2. The C at% and O/C ratio contents were again first investigated. The 15 min polymerization process showed a significant increase of O/C ratio from 0.2 (control) to 0.5. The oxygen content was overall found to sharply increase beyond 9 min. Upon deconvoluting the C 1s high resolution spectra, four main curves, corresponding to C-H, C-OR, C=O and COOH bonds, were assigned at 284.8, 286.3, 287.9 and 289.2 eV respectively [34, 35]. The relative increase visible for the C-O-R bonding including carbonyl (C-OR) and carboxylic (COOH) bonds densities visible in Figure 4C complies with the increase in oxygen elemental content as found in the survey spectra and previously introduced.

Furthermore, the impact of the functional groups generated upon plasma polymerization as a function of the process duration was also assessed by the measuring the surface charge by streaming potential for the series of samples. As seen in Figure 5A, the amine enrichment led to a sharp increase of the overall surface energy of the membrane materials, from -25 to -5 mV at pH 7. It also dramatically shifted the IEP from ~pH 3 for the control membrane to ~pH 7 +/- 0.5 pH unit for all plasma polymerization durations. The increased IEPs are supported by the XPS results, and indicate that a much higher density of amine moieties are readily available for protonation across the surface of the plasma polymerized membranes compared to the pristine membrane materials. Furthermore, the increase in the carboxylate moieties density for the MA plasma polymerized samples also led to major surface charge alterations, as shown in Figure 5B. The polymerization of MA led to a progressive and significant enhancement of the absolute negative charge of the membrane material. The surface charge of the membrane was found to be reduced reaching from – 20 mV (fresh control) to approximately -50 mV (5 and 9 min) and -80 mV (15 min) at pH 8. Interestingly, these

membranes exhibited a permanent negative charge across the pH range probed (3 to 8) which is highly relevant to seawater, brackish water or municipal wastewaters which are naturally in the pH range of 6 to 8. These results demonstrate that in addition to controlling the chemistry of the top layer of the material, such treatments allow for fine tuning of the surface charge of the materials by simply varying the plasma duration.

3.2 The influence of polymerized coating layers on performance of the membranes

The performance of the two series of membranes were evaluated without any pre-conditioning treatment in a cross-flow filtration system.

As shown in Figure 6A, the water flux after plasma polymerization with the VIM monomer was initially increased to 47.2 and 49.2 $L.m^{-2}.h^{-1}$after 5 and 9 min of treatment corresponding to 5 and 10 % increase, respectively, compared to the control membrane (44.9 $L.m^{-2}.h^{-1}$). Beyond 9 min, the values declined to a level comparable to that of the reference membranes (44.2 $L.m^{-2}.h^{-1}$), which was attributed to the increased mass transfer resistance of the membranes due to the thicker polymerized layer. In terms of selectivity, the salt rejection was maintained between 5 and 9 min (97.5 % and 97.0 % +/- 0.5 %) of plasma duration, respectively, but slightly declined (96 % +/- 0.4%) after 15 min of plasma duration, compared to the benchmark control membranes (98 % +/- 0.3 %). It is possible that the enhanced flux obtained for short plasma durations is directly related to mild physical etching of the surface of the materials as previously reported for plasma gas (DC) treatment of TFC membranes. A similar mechanism leading to the etching of the preservative may have etched nanometers of PA without generating subsequent changes of chemical functionalities.

The performance of the membranes plasma polymerized with MA is presented in Figure 6B. The water flux across the plasma polymerized membranes was slightly reduced to 41.4

$L.m^{-2}.h^{-}$ at 5 min of duration but significantly declined to 30.2 and 36.8 $L.m^{-2}.h^{-1}$ corresponding to 33% and 18% decline after 9 and 15 min of plasma duration, respectively. These stronger declines may be attributed to the thicker nature of the membranes, whose active layer was nearly doubled at such durations compared to the benchmark PA layer thickness. The salt rejection was maintained at 97.5% (+/- 0.5 %) for 5 and 9 min of process durations but slightly declined to 96.8% (+/- 0.3 %) after 15 min of duration. Similar impact on the flux associated with increasing film on the surface has been reported using conventional chemical routes for surface coating. In these studies, the surface of the membranes was coated with hydrophilic polymers which led to a flux decline of 25 - 81% depending on the thickness of the coated layers. In contrast with the present work, the exact modified film thickness was however not reported in these references [36, 37]. The performance of both the VIM and MA polymerized membrane series was plotted against the film thicknesses, Figure 7, and the flux may be seen to vary inversely with the layer thickness calculated from the FTIR data.

Although the selectivity of the membranes for specific ions was not investigated in this work, it is likely that amine or carboxylic groups enrichment would strongly alter specific selectivities for cations or anions, as shown in Figure 5, by changing the overall material charge and IEP [38]. The impact of ion valence on commercial RO membranes selectivities at different pH was previously investigated [8, 39]. Significant performance changes were obtained when dealing with selective diffusion of ions of largely different valence or hydrodynamic diameters, which was primarily attributed to combined change in Stern layer composition and thickness and to convective diffusion in the PA material [40]. Clear prospects from the current findings on plasma polymerized materials are that the selective polymerization and deposition mechanisms across the surface of the membranes may lead to highly selective membrane materials for resource recovery or selective RO ion diffusion. The customized charge approach could be applied to polyamide nanofiltration membranes, which are used widely for selective removal

and passage of small solutes, where charge of the membrane plays a critical role in their operation [8, 41]um.

4. Conclusions

This work investigated the impact of plasma polymerization on the performance of TFC membranes using two monomer models. The surface charge of the membranes was customized by altering the nature of the monomers and plasma durations used, in otherwise fixed plasma treatment and pre-conditioning conditions. The potential of plasma polymerization technologies to provide custom-engineered surfaces for TFC membranes is further evidenced by the fact that treatments performed under the most suitable conditions can improve performance in terms of flux, while maintaining the overall selectivity of the membrane.

Acknowledgement

Dr. DUMEE acknowledges Deakin University for his Alfred Deakin Post-Doctoral Fellowship (ADPDF2015). The support of the Australian Synchrotron for the beamtime M6419 on the IR spectroscopy beamline.

Figures and Tables

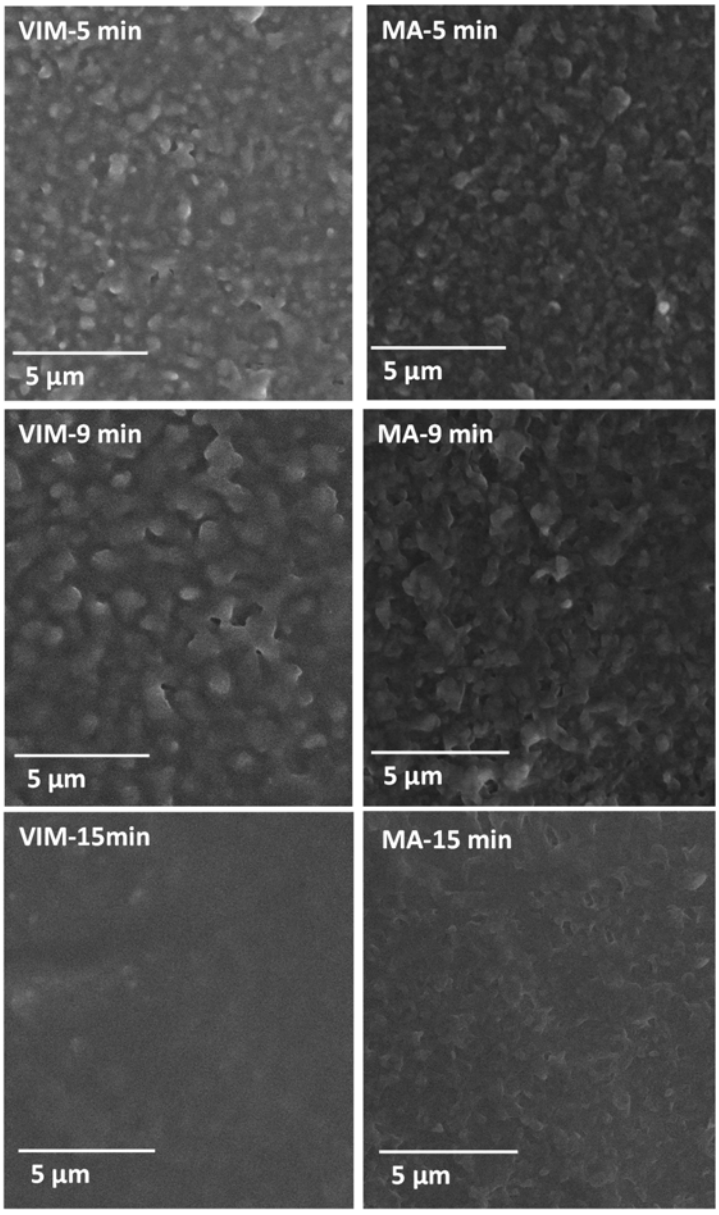

Figure 1 SEMs of the fresh control membrane onto which plasma polymerized membranes with VIM and MA were deposited using an AC plasma reactor and process durations of 5, 9 and 15 min. The SEM of the surface of the control membrane is provided in Figure S1

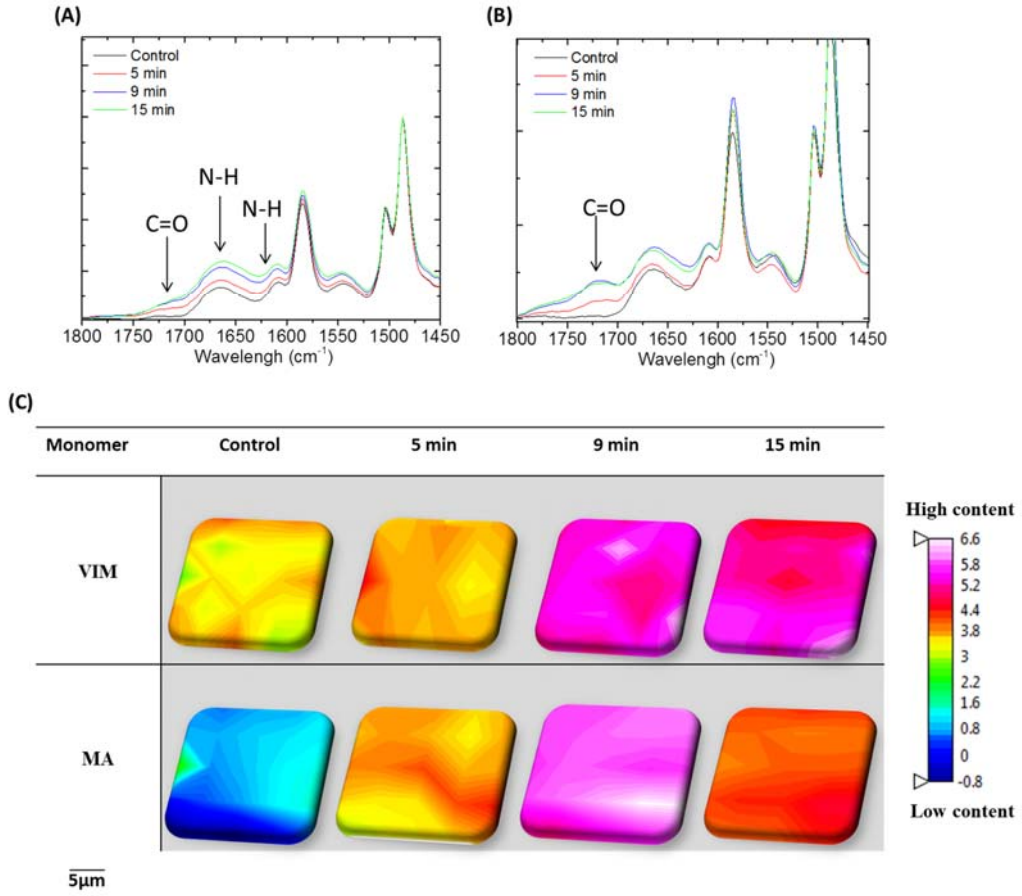

Figure 2 ATR-FTIR peak profile for absorption bands noted after plasma polymerization. Total of 25 points were measured in each map using an aperture of 20 x 20 µm with spot size of 5 µm and distance between points of 2.5 µm. a) plasma polymerization with VIM: reference band at 1666 cm^{-1}. b) plasma polymerization with MA: reference band at 1722 cm^{-1} and c) homogeneity analysis on 5 µm x 5 µm maps with integration of bands around 1666 cm^{-1} and 1722 cm^{-1}

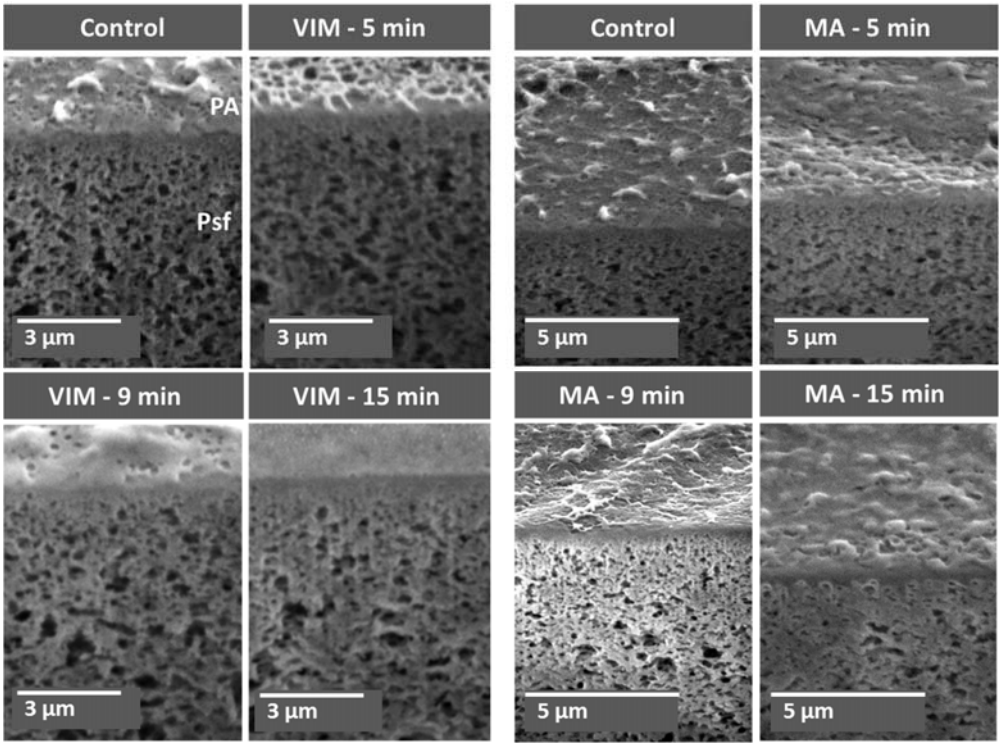

Figure 3 SEM cross-sections made by FIB milling of the membranes. The variation in polymerized layer thicknesses may be visualized at the interface of the PA layer

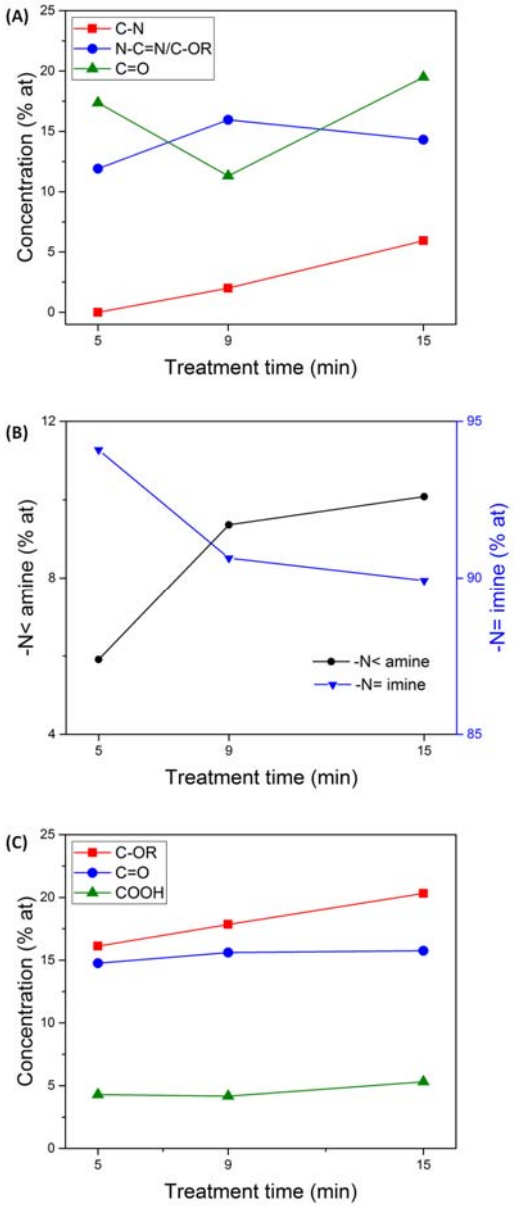

Figure 4 XPS analysis of the surface of both VIM and MA plasma polymerized samples. Reference spectra for the control membranes are provided in the supplementary information. (A) Concentration of C-N, N-C=N or C-OR and C=O bonds for the VIM polymerized samples at different plasma polymerized durations; (B) Corresponding amine and imide ratios and (C) Concentrations of C-OR, C=O and COOH across the MA polymerized samples. The raw data and fittings for each specific functional bond are provided in Figure S2

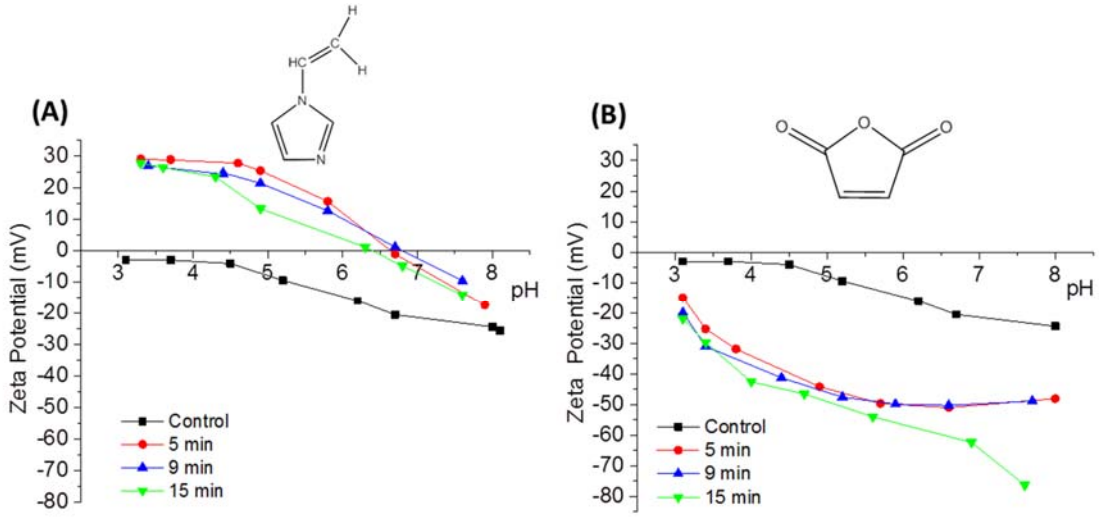

Figure 5 Surface charge analysis of fresh plasma polymerized membranes a) plasma polymerization with VIM and b) plasma polymerization with MA

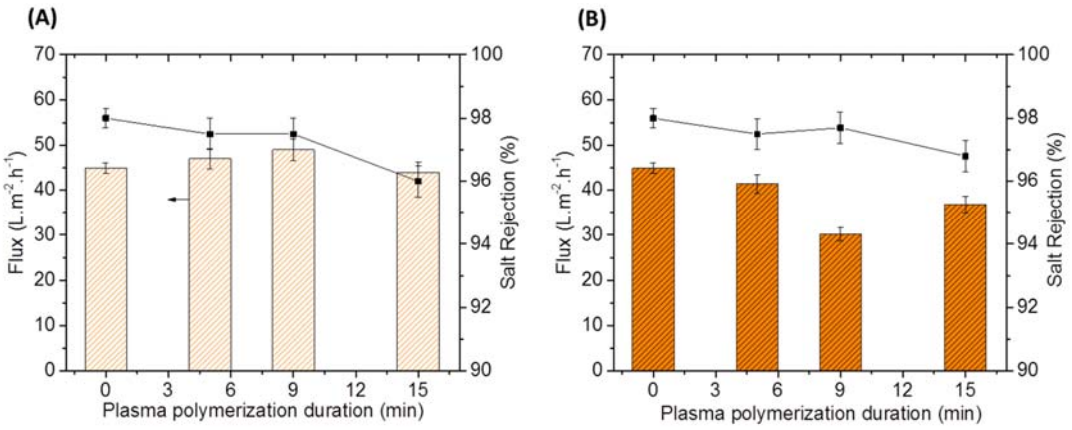

Figure 6 Permeation tests of membranes after plasma polymerization under 15 bar inlet pressure and 2,000 ppm NaCl solution, 27ºC at pH 6.5. a) VIM polymerization and b) MA polymerization performed at 5, 9 and 15 min polymerization duration

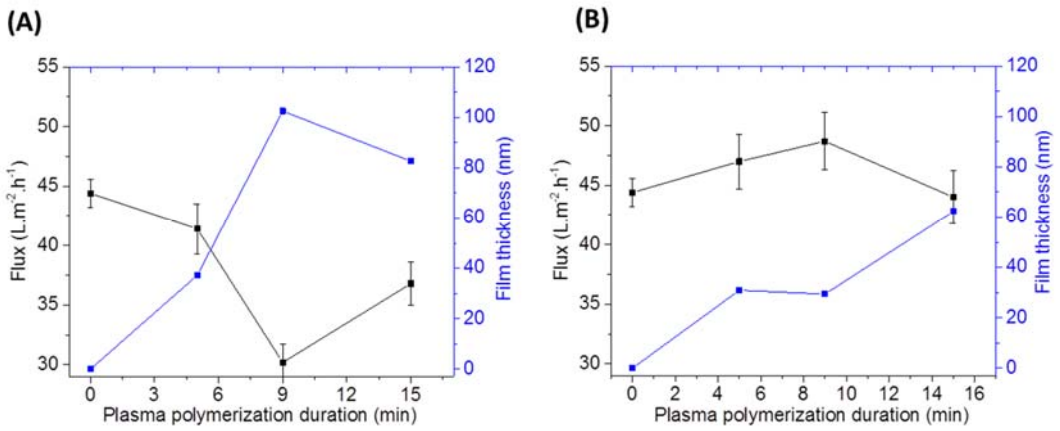

Figure 7 Correlation between polymerized film thickness and water flux a) plasma polymerization with MA and b) plasma polymerization with VIM

Supplementary material

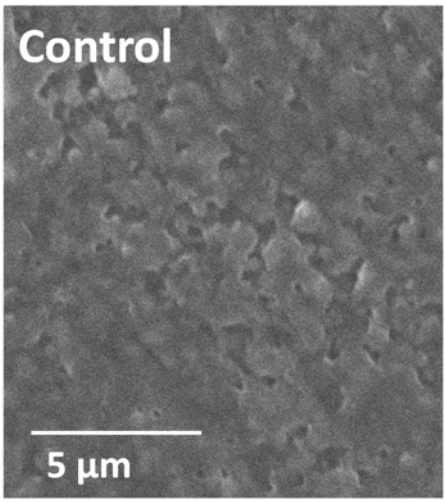

Figure S1 SEM of the surface of the reference BW30 membrane

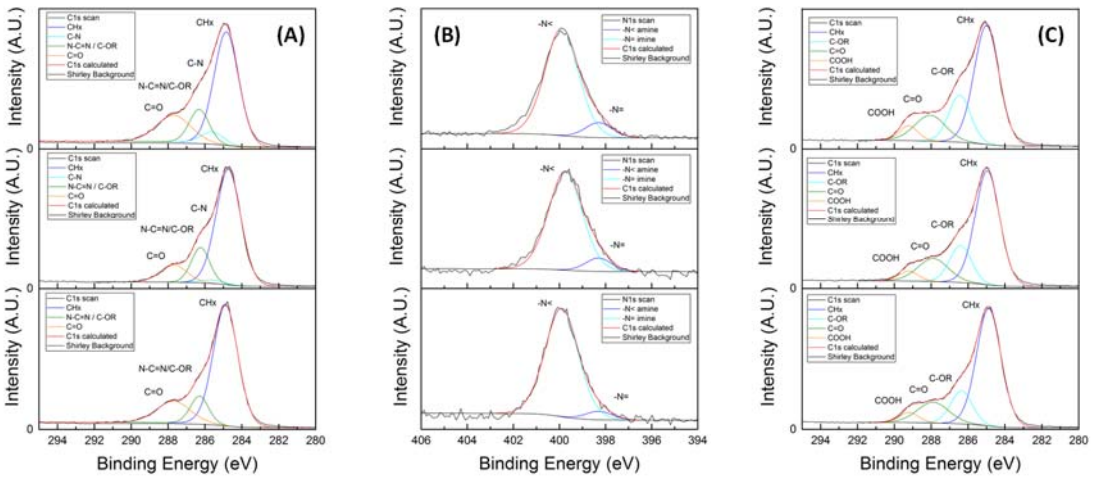

Figure S2 XPS peak deconvolutions for the VIM (A) Carbon and (B) Nitrogen spectra as well as for the MA (C) Carbon spectrum. The sum of the fittings, to highlight the residual trace are provided as the red line across the black, continuous, thin line of the initial spectra. Atomic ratios and overall compositions are provided in Table S1

Table S1 XPS contents from fresh plasma polymerized membranes with VIM and MA monomers. The errors correspond to standard deviations from 3 measurements in each sample

Membranes	C (at%)	N (at%)	O (at%)	S (at%)	N/C	O/C
Control	76.5 ± 0.5	5.5 ± 0.2	18.2 ± 0.3	0	0.07	0.24
VIM-5 min	75.5 ± 3.5	11 ± 2.5	13 ± 0.9	0.5 ± 0.1	0.14	0.17
VIM-9 min	73.1 ± 0.9	13.3 ± 0.8	13.2 ± 0.1	0.4 ± 0.1	0.18	0.18
VIM-15 min	75 ± 0.4	11.2 ± 0.8	13.6 ± 0.2	0.3 ± 0.1	0.15	0.18
MA-5 min	77.2 ± 2	3.2 ± 0.3	19.3 ± 2	0.3 ± 0.1	0.04	0.25
MA-9 min	80.2 ± 1.3	2.6 ± 0.6	16.7 ± 0.8	0.5 ± 0.1	0.03	0.21
MA-15 min	63.0 ± 0.6	1.9 ± 0.1	30.7 ± 0.8	2.3 ± 0.1	0.03	0.48

References

1. L. F. Greenlee, D. F. Lawler, B. D. Freeman, B. Marrot and P. Moulin, *Water research*, 2009, **43**, 2317-2348.

2. K. P. Lee, T. C. Arnot and D. Mattia, *Journal of Membrane Science*, 2011, **370**, 1-22.

3. L. Dumée, J. Lee, K. Sears, B. Tardy, M. Duke and S. Gray, *Journal of membrane science*, 2013, **427**, 422-430.

4. X. Lu, C. Boo, J. Ma and M. Elimelech, *Environmental Science & Technology*, 2014, **48**, 14369-14376.

5. A. E. Childress and M. Elimelech, *Journal of Membrane Science*, 1996, **119**, 253-268.

6. D. Li, Y. Yan and H. Wang, *Progress in Polymer Science*, 2016, **61**, 104-155.

7. L. He, L. F. Dumée, C. Feng, L. Velleman, R. Reis, F. She, W. Gao and L. Kong, *Desalination*, 2015, **365**, 126-135.

8. M. Mullett, R. Fornarelli and D. Ralph, *Membranes*, 2014, **4**, 163-180.

9. C. Y. Tang, T. H. Chong and A. G. Fane, *Advances in colloid and interface science*, 2011, **164**, 126-143.

10. A. Fridman, *Journal*, 2008.

11. M. Chaudhuri, A. V. Ivlev, S. A. Khrapak, H. M. Thomas and G. E. Morfill, *Soft Matter*, 2011, **7**, 1287-1298.

12. K. C. Khulbe, C. Feng and T. Matsuura, *Journal of Applied Polymer Science*, 2010, **115**, 855-895.

13. L.-S. Wan, Z.-M. Liu and Z.-K. Xu, *Soft Matter*, 2009, **5**, 1775-1785.

14. E.-S. Kim and B. Deng, *Membrane Water Treatment*, 2013, **4**, 109-126.

15. S. Wu, J. Xing, C. Zheng, G. Xu, G. Zheng and J. Xu, *Journal of Applied Polymer Science*, 1997, **64**, 1923-1926.

16. J. Albo, J. Wang and T. Tsuru, *Journal of Membrane Science*, 2014, **453**, 384-393.

17. M. C. Porter, *Handbook of industrial membrane technology*, Noyes Publications, New Jersey, 1989 pp-143.

18. D. Filmtec, Handling, Preservation and Storage: Re-wetting of Dried Out Elements Home Page.http://www.dowwaterandprocess.com/en/resources/reverse-osmosis-technical-manual (accessed March, 2014)).

19. R. Reis, L. F. Dumee, L. He, F. She, J. D. Orbell, B. Winther-Jensen and M. C. Duke, *ACS applied materials & interfaces*, 2015, **7**, 14644-14653.

20. K. Norrman and B. Winther-Jensen, *Plasma Processes Polym.*, 2005, **2**, 414-423.

21. M. Cantini, P. Rico, D. Moratal and M. Salmeron-Sanchez, *Soft Matter*, 2012, **8**, 5575-5584.

22. H. K. Yasuda, *Plasma Processes Polym.*, 2005, **2**, 293-304.

23. L. F. Dumée, L. He, P. C. King, M. Le Moing, I. Güller, M. Duke, P. D. Hodgson, S. Gray, A. J. Poole and L. Kong, *Journal of Membrane Science*, 2015, **475**, 552-561.

24. C. Y. Tang, Y.-N. Kwon and J. O. Leckie, *Journal of Membrane Science*, 2007, **287**, 146-156.

25. C. Y. Tang, Y.-N. Kwon and J. O. Leckie, *Desalination*, 2009, **242**, 149-167.

26. A. Merenda, E. des Ligneris, K. Sears, T. Chaffraix, K. Magniez, D. Cornu, J. A. Schütz and L. F. Dumée, *Scientific Reports*, 2016, **6**.

27. M. M. Hossain, *Plasma technology for deposition and surface modification*, Logos Verlag Berlin GmbH, 4 (2009) 55-56.

28. H. Yasuda, *Plasma polymerization* Academic Press, INC, Orlando, Florida 32887, 1(1985) 82-83.

29. S. Yuan, S. O. Pehkonen, B. Liang, Y. P. Ting, K. G. Neoh and E. T. Kang, *Corrosion Science*, 2010, **52**, 1958-1968.

30. W. H. Yu, Y. Zhang, E. T. Kang, K. G. Neoh, S. Y. Wu and Y. F. Chow, *Journal of The Electrochemical Society*, 2002, **149**, C521-C528.

31. G. Yang, E. Kang, K. Neoh, Y. Zhang and K. Tan, *Langmuir*, 2001, **17**, 211-218.

32. R. Reis, L. F. Dumée, B. L. Tardy, R. Dagastine, J. D. Orbell, J. A. Schutz and M. C. Duke, *Scientific Reports*, 2016, **6**, 29206.

33. K. L. Tu, A. R. Chivas and L. D. Nghiem, *Journal of Membrane Science*, 2014, **472**, 202-209.

34. P. Stenstad, M. Andresen, B. S. Tanem and P. Stenius, *Cellulose*, 2008, **15**, 35-45.

35. M. Andresen, L.-S. Johansson, B. S. Tanem and P. Stenius, *Cellulose*, 2006, **13**, 665-677.

36. J. S. Louie, I. Pinnau, I. Ciobanu, K. P. Ishida, A. Ng and M. Reinhard, *J. Membr. Sci.*, 2006, **280**, 762-770.

37. J. Gilron, S. Belfer, P. Vaisanen and M. Nystrom, *Desalination*, 2001, **140**, 167-179.

38. W. Gao, F. She, J. Zhang, L. F. Dumée, L. He, P. D. Hodgson and L. Kong, *Journal of Membrane Science*, 2015, **487**, 32-39.

39. K. Kezia, J. Lee, W. Ogieglo, A. Hill, N. E. Benes and S. E. Kentish, *Journal of Membrane Science*, 2014, **459**, 197-206.

40. O. Nir, N. F. Bishop, O. Lahav and V. Freger, *Water research*, 2015, **87**, 328-335.

41. J. Lim, C. Scholes, L. Dumée and S. Kentish, *International journal of greenhouse gas control*, 2014, **30**, 34-41.